MATERIALE PLASTICE
https://revmaterialeplastice.ro
https://doi.org/10.37358/Mat.Plast.1964

Theoretical Prediction of Two-Peak Behavior of GFRP-Reinforced Concrete Compressive Members

MOHAMED HECHMI EL OUNI[1, 2], ALI RAZA[3*], MUHAMMAD ARSHAD[3]
[1]Department of Civil Engineering, College of Engineering, King Khalid University, PO Box 394, Abha 61411 Kingdom of Saudi Arabia
[2]Department of Mechanical Engineering, Higher Institute of Applied Sciences and Technologies of Sousse, University of Sousse, 4003, Sousse Ibn Khaldoun, Tunisia
[3]Department of Civil Engineering, University of Engineering and Technology Taxila, 47050, Pakistan

Abstract: *The use of fiber-reinforced polymer (FRP) composites in compressive members is advantageous to reinforced concrete structures in order to alleviate the problem of corrosion of steel reinforcement and to produce a lightweight and efficient structural element. This investigation aims to propose the theoretical models for capturing the axial loading capacity (ALC) of hollow concrete columns (HCCs) having main FRP rebars and transverse FRP spirals. All the glass-FRP-reinforced HCCs portray two-peak load performance. The first peak is due to the gross cross-sectional area of concrete while the second peak is due to the core material laterally wrapped with FRP spirals. For the prediction of the first peak load of HCCs which is equal to the maximum capacity of solid concrete columns, a database of 279 FRP-reinforced columns was produced from the previous research and the ALC models were suggested; one for capturing the first peak and the other for estimating the second peak ALC of HCCs. The predictions of proposed models were compared with the test results from the literature. A close relationship was perceived between the theoretical and experimental results.*

Keywords*: hallow concrete columns, glass-FRP spirals, wrapping, axial capacity, analytical model*

1.Introduction

When compared with solid concrete compressive members, hollow concrete columns (HCCs) offer more resistance to axial loads and moments. Having higher structural efficacy and increased stiffness to mass ratios these columns are generally preferred due to their economic designs and lighter weights [1, 2]. In addition, as alternative to solid concrete piers, HCCs are more economical for their support as bridge piers. Reducing the influence of the column's masses on the seismic behavior minimizes the load-carrying demands on the underlying subsurface structure [3]. Over the years, scholars have been examining the efficacy of HCCs coupled with steel bars under varying load conditions [1, 2, 4-11]. With these studies, researchers concluded not only the efficient behavior of HCCs is governed primarily on the interior to the external diameter ratios of the HCCs but also, different ratios such as axial-loadings, main reinforcements, and the transverse detailing also play their key role. Likewise, increasing i/o when remaining all the other parameters are kept as constant, reinforced HCCs become less ductile. A drastic fall in axial compressive strength occurred when the ultimate capacity is achieved. This loss in strength was observed more pronounced in HCCs having larger i/o ratios. [5, 12]. Because of failures due to buckling and limited steel strains in their axial direction, HCCs were not evaluated in their post-loading stages. As a replacement, when buckling of steel bars starts, concrete gets crushed [1, 13, 14].

Corrosion, being one of the major concerns in HCCs due to the smaller cover of concrete and thinner steel reinforcing walls when compared to those of solid concrete columns, decreases the loading capacities of HCCs by eradicating and damaging the wrappings placed in transverse directions of steel bars [15, 16]. Currently, the majority of HCC bridges are being strengthened again to achieve their desired serviceability [3, 13]. Therefore, non-corroding materials are making their way by overwhelming the axial strengths as well as strains of HCCs. Because of their frequent use, Fiber-reinforced polymers (FRPs) are also placed as internal reinforcements and / or exterior wrappings during the manufacturing

**email:ali.raza@uettaxila.edu.pk*

of recently built structures. In addition, their application to strengthen and/or retrofit the built structures are unlimited [17-20]. In recent times, glass FRPs (glass-FRPs) are also employed as main as well as transverse wrappings in different columns [21-31]. Studies conclude that the glass-FRP reinforced concrete columns (RCC) under axial loads perform better when subjected to their peak compressive strengths of concrete members. Because of their linear elastic behavior glass-FRP bars tend to have higher strength without loss of stiffness up to failure stage by making them more efficient for their lateral wrapping phenomenon.

During an investigation carried out by Mohamed et al. [32], researchers evaluated fourteen full-scale FRP-RCC members subjected to axial loads. Columns failed at reduced volumetric ratios of lateral reinforcement (0.7%), main bars buckled. However, at a moderate level of ratios, columns with lateral reinforcements (1.5% and 2.7%), failed by rupturing the lateral wrappings ultimately leading to crushing the concrete cores. Afifi et al. [33] suggested models for concretes with glass-FRP wrappings by calibrating it with the regression analysis on the experimented findings to predict the axial loading capacity (ALC) and specimens' strains. Moreover, 800 mm reinforced glass-FRP samples with 12 in numbers having 205 mm diameter were evaluated by Hadi et al. [24] under varying scenarios of the loadings. They concluded that the ALC of glass-FRP-RC samples was observed smaller when compared with those of steel-RC counterparts. Additionally, a higher level of discrepancy between the tested and theoretical estimates of columns capacities was observed when the influence of glass-FRP bars was neglected during compression in axial directions. Karim et al. [30] proposed another model to estimate the load-deflection behavior of spiral-wrapped glass-FRP-RC samples. It was observed that the FRP-wrapped specimens presented a two-peak axial loading performance: the first peak represents the capacity of the gross cross-section of concrete material and the second represents the capacity of FRP-wrapped concrete core. During another study, AlAjarmeh et al. [27] observed HCCs coupled with glass-FRP bars and found significant improvement in the axial strengths, wrapping efficiencies as well as axial strains of HCCs when amount as well as diameter of glass-FRP rebars was increased. Using more glass-FRP rebars having lesser diameter, this efficiency enhanced up to 12%. In addition, the axial strength of HCCs with glass-FRP were predicted with more accuracy the effect of glass-FRP bars was considered.

The main objective of the present work is to suggest novel empirical models predict the peak loadings of HCCs with glass-FRP bars. To meet the intended goal, a complete database with 279 FRP-reinforced members was devised using the available literature. To attain a more generic form of the model being proposed, preliminary evaluations of already published models were carried out. Later on, two models were proposed to predict the first as well as second peak loads (SPL) of glass-FRP-strengthened HCCs. It is believed that this study will pose an utmost impact for analysis and designs of HCCs with glass-FRP bars when employed as transverse and main reinforcement.

2.Materials and methods

2.1. Theoretical capacity

Though numerous researchers [21-24] revealed that glass-FRP rebars should be considered to predict the axial strength, due to limited experimentations and literature available, ACI [34] and CSA [35] do not keep this observation of glass-FRP contribution to compute the column's ALC. Moreover, glass-FRP-based HCCs showed two-peak behavior during their loadings [24, 27, 28]. The first peak is obtained during the stage when the capacity of the gross cross-sectional area (CSA) is wrapped with glass-FRP spirals. SPL (P_{n2}) is obtained because the ultimate ALC of the concrete core is restricted with glass-FRP spirals [24]. Also, the first peak capacities are the same for both HCCs and solid [27]. Consequently, this study aims to propose an empirical model for the first peak loads (FPL) utilizing the database developed for FRP-RCC columns and the SPL projected by initiating the phenomenon of wrapping developments and experimental pieces of evidence of glass-FRP-strengthened HCCs [27, 28].

2.1.1. First peak capacity

2.1.1.1. Developed database

Utilizing the findings of two hundred and seventy-nine FRP-RCC from the published literature including the geometric and physical characteristics of the specimens. The transverse reinforcement in the specimens was either kept as steel/FRP spirals or hoops, but it was found that such variations do not affect the prediction of the first peak capacities. 133 specimens in rectangular shape and 146 in the circular formation of columns were assessed. The database contained all necessary parameters including but not limited to CSA, compressive and tensile strengths and tensile strengths of FRPs, their elastic modulus values, maximum tested and available tensile strains, FRP reinforcement ratios, transverse reinforcement ratio, and first peak column capacities. This information derived from the database is shown in Table 1.

Table 1. Database outline

Research study	Ag (mm^2)	fc' (MPa)	f_u (MPa)	E_f (GPa)	ε_u *(%)*	ρ_l *(%)*	A_f (mm^2)	Ties	ρ_t *(%)*	P_{n1} (kN)
Afifi et al. [36]	70650	20	934	55.4	1.56	2.2	1567.74	GS	1.00	2920
Afifi et al. [36]	70650	20	934	55.4	1.56	1.1	783.87	GS	1.00	2826
Afifi et al. [36]	70650	20	934	55.4	1.56	3.2	2351.61	GS	1.00	2998
Afifi et al. [36]	70650	20	934	55.4	1.56	2.2	1567.74	GS	0.45	2857
Afifi et al. [36]	70650	20	934	55.4	1.56	2.2	1567.74	GS	1.87	3019
Afifi et al. [36]	70650	20	934	55.4	1.56	2.2	1567.74	GS	2.07	2964
Afifi et al. [36]	70650	20	934	55.4	1.56	2.2	1567.74	GS	0.69	2804
Afifi et al. [36]	70650	20	934	55.4	1.56	2.2	1567.74	GS	1.03	2951
Afifi et al. [36]	70650	20	934	55.4	1.56	2.2	1567.74	GS	1.03	2865
Afifi et al. [37]	71121	21	934	55.4	1.56	2.2	1567.74	GS	1.50	2840
Afifi et al. [37]	71595	22	934	55.4	1.56	2.2	1567.74	GS	1.50	2871
Afifi et al. [37]	72070	23	934	55.4	1.56	2.2	1567.74	GS	1.50	2935
AlAjarmeh et al. [38]	49062	31.8	1237	60	2.1	2.41	1175.80	GS	1.49	1588
AlAjarmeh et al. [38]	49062	31.8	1237	60	2.1	2.47	1175.80	GS	1.56	1408
AlAjarmeh et al. [38]	49062	31.8	1237	60	2.1	2.59	1175.80	GS	1.69	1559
AlAjarmeh et al. [38]	49062	31.8	1237	60	2.1	2.78	1175.80	GS	1.92	1411
AlAjarmeh et al. [39]	49455	25	1281.5	61.3	2.1	1.78	759.68	GS	1.57	1035.3
AlAjarmeh et al. [39]	49850	25	1237.4	60.5	2.1	2.79	1175.80	GS	1.57	1109.2
AlAjarmeh et al. [39]	50247	25	1270	60.5	2.1	4	1700.31	GS	1.57	1247.9
AlAjarmeh et al. [39]	50645	25	1237.4	60.5	2.1	1.86	783.87	GS	1.57	983.3
AlAjarmeh et al. [39]	51044	25	1237.4	60.5	2.1	3.72	1567.74	GS	1.57	1406.1
AlAjarmeh et al. [39]	51445	25	1281.5	61.3	2.1	2.67	1139.51	GS	1.57	1204.2
Alsayed et al. [40]	112500	39	800	40	1.5	1	1175.80	SH	0.15	3285
Alsayed et al. [40]	112500	39	800	40	1.5	1	1175.80	SH	0.15	3285
Alsayed et al. [40]	112500	39	800	40	1.5	1	1175.80	SH	0.15	3285
Alsayed et al. [40]	112500	38.5	800	40	1.5	1	1175.80	GH	0.18	3301
Alsayed et al. [40]	112500	38.5	800	40	1.5	1	1175.80	GH	0.18	3301
Alsayed et al. [40]	112500	38.5	800	40	1.5	1	1175.80	GH	0.18	3301
De Luca et al. [41]	372100	43.7	608	44.2	1.38	1	4051.60	GH	0.63	15235
De Luca et al. [41]	372100	40.6	712	44.4	1.6	1	4051.60	GH	0.63	12949
De Luca et al. [41]	372100	36.1	608	44.2	1.38	1	4051.60	GH	2.5	11926
De Luca et al. [41]	372100	32.8	712	44.4	1.6	1	4051.60	GH	2.5	10751

Dong et al. [42]	36286	40	930	59	1.6	0.55	212.54	GS	0.94	1018
Dong et al. [42]	36286	40	930	59	1.6	0.73	283.39	GS	0.94	1179
Dong et al. [42]	36286	40	930	59	1.6	0.92	354.23	GS	0.94	1288
Dong et al. [42]	36286	40	930	59	1.6	1.1	425.08	GS	0.94	1381
Dong et al. [42]	36286	40	930	59	1.6	0.73	283.39	GS	2.75	1459
Dong et al. [42]	36286	40	930	59	1.6	0.73	283.39	GS	2.75	1037
Dong et al. [42]	36286	40	880	59	1.6	0.73	283.39	GS	2.75	523
Dong et al. [42]	36286	37	880	59	1.6	0.73	283.39	GS	2.75	318
Dong et al. [42]	36286	37	880	59	1.6	0.73	354.23	GS	1.39	1290
Dong et al. [42]	36286	37	880	59	1.6	0.73	425.08	GS	1.39	944
Dong et al. [42]	36286	37	880	59	1.6	0.73	495.92	GS	1.39	527
Dong et al. [42]	36286	37	880	59	1.6	0.73	566.77	GS	1.39	296
Elchalakani and Ma [43]	41600	32.8	1200	50	2.4	1.8	759.68	GH	0.5	1367
Elchalakani and Ma [43]	41600	32.8	1200	50	2.4	1.8	759.68	GH	0.5	880
Elchalakani and Ma [43]	41600	32.8	1200	50	2.4	1.8	759.68	GH	0.5	584
Elchalakani and Ma [43]	41600	32.8	1200	50	2.4	1.8	759.68	GH	1.0	1449
Elchalakani and Ma [43]	41600	32.8	1200	50	2.4	1.8	759.68	GH	1.0	917
Elchalakani and Ma [43]	41600	32.8	1200	50	2.4	1.8	759.68	GH	1.0	788
Elchalakani and Ma [43]	41600	32.8	1200	50	2.4	1.8	759.68	GH	0.3	1402
Elchalakani and Ma [43]	41600	32.8	930	59	1.7	1.8	759.68	GH	0.3	1402
Elchalakani and Ma [43]	41600	32.8	930	59	1.7	1.8	759.68	GH	0.5	1367
Elchalakani and Ma [43]	41600	32.8	930	59	1.7	1.8	759.68	GH	1.0	1449
Elchalakani and Ma [43]	41600	32.8	930	59	1.7	1.8	759.68	GH	0.5	880
Elchalakani and Ma [43]	41600	32.8	930	59	1.7	1.8	759.68	GH	1.0	917
Elchalakani and Ma [43]	41600	32.8	930	59	1.7	1.8	759.68	GH	1.0	788
Elchalakani and Ma [43]	41600	32.8	930	59	1.7	1.8	759.68	GH	0.5	584
Elchalakani and Ma [43]	41600	32.8	930	59	1.7	1.8	759.68	GH	0.3	1041
Elchalakani and Ma [43]	41600	32.8	930	59	1.7	1.8	759.68	GH	0.5	1194
Elchalakani and Ma [43]	41600	32.8	930	59	1.7	1.8	759.68	GH	1.0	1357
Elchalakani and Ma [43]	41600	32.8	930	59	1.7	1.8	759.68	GH	0.5	657
Elchalakani and Ma [43]	41600	32.8	930	59	1.7	1.8	759.68	GH	1.0	804
Elchalakani and Ma [43]	25600	32.8	930	59	1.7	1.8	759.68	GH	0.5	353
Elchalakani and Ma [43]	25600	32.8	930	59	1.7	1.8	759.68	GH	1.0	454
Elchalakani and Ma [43]	25600	32.8	930	59	1.7	1.8	759.68	GH	0.5	234
Elchalakani and Ma [43]	25600	32.8	930	59	1.7	1.8	759.68	GH	1.0	244
Guerin et al. [44]	164025	25.3	600	40	1.5	1	1700.31	GH	0.66	4587
Guerin et al. [44]	164025	25.3	600	40	1.5	1	1700.31	GH	0.66	3433
Guerin et al. [44]	164025	25.3	600	40	1.5	1	1700.31	GH	0.66	1591
Guerin et al. [44]	164025	25.3	600	40	1.5	1	1700.31	GH	0.66	645
Guerin et al. [44]	164025	25.3	600	40	1.5	1	1700.31	GH	0.66	4616
Guerin et al. [44]	164025	25.3	600	40	1.5	1	1700.31	GH	0.66	3405
Guerin et al. [44]	164025	25.3	600	40	1.5	1	1700.31	GH	0.66	1576
Guerin et al. [44]	164025	25.3	600	40	1.5	1	1700.31	GH	0.66	636
Guerin et al. [45]	164025	25.3	600	40	1.5	1.4	2267.08	GH	0.84	5028
Guerin et al. [45]	164025	25.3	600	40	1.5	1.4	2267.08	GH	0.84	3627

Guerin et al. [45]	164025	25.3	600	40	1.5	1.4	2267.08	GH	0.84	2035
Guerin et al. [45]	164025	25.3	600	40	1.5	1.4	2267.08	GH	0.84	914
Guerin et al. [45]	164025	25.3	600	40	1.5	2.5	4051.60	GH	0.63	5294
Guerin et al. [45]	164025	25.3	600	40	1.5	2.5	4051.60	GH	0.63	3790
Guerin et al. [45]	164025	25.3	600	40	1.5	2.5	4051.60	GH	0.63	2110
Guerin et al. [45]	164025	25.3	600	40	1.5	2.5	4051.60	GH	0.63	1008
Hadhood et al. [46]	73024	35	1680	141	1.19	2.2	1567.74	GH	2.68	2564
Hadhood et al. [46]	73024	35	1680	141	1.19	2.2	1567.74	GH	2.68	2060
Hadhood et al. [46]	73024	35	1680	141	1.19	2.2	1567.74	GH	2.68	1511
Hadhood et al. [46]	73024	35	1680	141	1.19	2.2	1567.74	GH	2.68	776
Hadhood et al. [46]	73024	35	1680	141	1.19	2.2	1567.74	GH	2.68	366
Hadhood et al. [46]	73024	35	1680	141	1.19	2.2	1567.74	GS	1.0	2608
Hadhood et al. [46]	73024	35	1680	141	1.19	2.2	1567.74	GS	1.0	2134
Hadhood et al. [46]	73024	35	1680	141	1.19	2.2	1567.74	GS	1.0	1513
Hadhood et al. [46]	73024	35	1680	141	1.19	2.2	1567.74	GS	1.0	745
Hadhood et al. [46]	73024	35	1680	141	1.19	2.2	1567.74	GS	1.0	654
Hadhood et al. [46]	73024	35	1680	141	1.19	3.3	2351.61	GS	1.0	2670
Hadhood et al. [46]	73024	35	1680	141	1.19	3.3	2351.61	GS	1.0	2123
Hadhood et al. [46]	73024	35	1680	141	1.19	3.3	2351.61	GS	1.0	1527
Hadhood et al. [46]	73024	35	1680	141	1.19	3.3	2351.61	GS	1.0	852
Hadhood et al. [46]	73024	35	1680	141	1.19	3.3	2351.61	GS	1.0	378
Hadhood et al. [47]	73024	35	1680	141	1.19	2.2	1567.74	GS	1.8	2652
Hadhood et al. [47]	73024	35	1680	141	1.19	2.2	1567.74	GS	1.8	2086
Hadhood et al. [47]	73024	35	1680	141	1.19	2.2	1567.74	GS	1.8	1483
Hadhood et al. [47]	73024	35	1680	141	1.19	2.2	1567.74	GS	1.8	747
Hadhood et al. [47]	73024	35	1680	141	1.19	2.2	1567.74	GS	1.8	655
Hadhood et al. [47]	73024	70.2	1289	54.9	2.3	2.2	1567.74	GS	1.1	4709
Hadhood et al. [47]	73024	70.2	1289	54.9	2.3	2.2	1567.74	GS	1.1	3309
Hadhood et al. [47]	73024	70.2	1289	54.9	2.3	2.2	1567.74	GS	1.1	2380
Hadhood et al. [47]	73024	70.2	1289	54.9	2.3	2.2	1567.74	GS	1.1	1112
Hadhood et al. [47]	73024	70.2	1289	54.9	2.3	2.2	1567.74	GS	1.1	797
Hadhood et al. [47]	73024	70.2	1289	54.9	2.3	2.2	1567.74	GH	1.1	4689
Hadhood et al. [47]	73024	70.2	1289	54.9	2.3	2.2	1567.74	GH	1.1	3299
Hadhood et al. [47]	73024	70.2	1289	54.9	2.3	2.2	1567.74	GH	1.1	2435
Hadhood et al. [47]	73024	70.2	1289	54.9	2.3	2.2	1567.74	GH	1.1	1054
Hadhood et al. [47]	73024	70.2	1289	54.9	2.3	2.2	1567.74	GH	1.1	838
Hadhood et al. [47]	73024	70.2	1289	54.9	2.3	3.2	2351.61	GS	1.1	4716
Hadhood et al. [47]	73024	70.2	1289	54.9	2.3	3.2	2351.61	GS	1.1	3380
Hadhood et al. [47]	73024	70.2	1289	54.9	2.3	3.2	2351.61	GS	1.1	2339
Hadhood et al. [47]	73024	70.2	1289	54.9	2.3	3.2	2351.61	GS	1.1	1135
Hadhood et al. [47]	73024	70.2	1289	54.9	2.3	3.2	2351.61	GS	1.1	713
Hadhood et al. [47]	73024	70.2	1289	54.9	2.3	2.2	1567.74	GS	1.1	5120
Hadhood et al. [47]	73024	70.2	1289	54.9	2.3	2.2	1567.74	GS	1.1	3671
Hadhood et al. [47]	73024	70.2	1289	54.9	2.3	2.2	1567.74	GS	1.1	2538
Hadhood et al. [47]	73024	70.2	1289	54.9	2.3	2.2	1567.74	GS	1.1	1392

Hadhood et al. [47]	73024	70.2	1289	54.9	2.3	2.2	1567.74	GS	1.1	611
Hadhood et al. [47]	73024	70.2	1289	54.9	2.3	2.2	1567.74	GS	1.7	4680
Hadhood et al. [47]	73024	70.2	1289	54.9	2.3	2.2	1567.74	GS	1.7	3341
Hadhood et al. [47]	73024	70.2	1289	54.9	2.3	2.2	1567.74	GS	1.7	2460
Hadhood et al. [47]	73024	70.2	1289	54.9	2.3	2.2	1567.74	GS	1.7	1061
Hadhood et al. [47]	73024	70.2	1289	54.9	2.3	2.2	1567.74	GS	1.7	682
Hadhood et al. [47]	73024	35	1289	54.9	2.3	2.2	1567.74	GS	1.1	2608
Hadhood et al. [47]	73024	35	1289	54.9	2.3	2.2	1567.74	GS	1.1	2134
Hadhood et al. [47]	73024	35	1289	54.9	2.3	2.2	1567.74	GS	1.1	1512
Hadhood et al. [47]	73024	35	1289	54.9	2.3	2.2	1567.74	GS	1.1	745
Hadhood et al. [47]	73024	35	1289	54.9	2.3	2.2	1567.74	GS	1.1	354
Hadhood et al. [47]	73024	35	1289	54.9	2.3	2.2	1567.74	GS	1.1	3090
Hadhood et al. [47]	73024	35	1289	54.9	2.3	2.2	1567.74	GS	1.1	2342
Hadhood et al. [47]	73024	35	1289	54.9	2.3	2.2	1567.74	GS	1.1	1746
Hadhood et al. [47]	73024	35	1289	54.9	2.3	2.2	1567.74	GS	1.1	995
Hadhood et al. [47]	73024	35	1289	54.9	2.3	2.2	1567.74	GS	1.1	529
Hadhood et al. [47]	73024	35	1289	54.9	2.3	2.2	1567.74	GS	1.1	2652
Hadhood et al. [47]	73024	35	1289	54.9	2.3	2.2	1567.74	GS	1.1	2086
Hadhood et al. [47]	73024	35	1289	54.9	2.3	2.2	1567.74	GS	1.1	1483
Hadhood et al. [47]	73024	35	1289	54.9	2.3	2.2	1567.74	GS	1.1	747
Hadhood et al. [47]	73024	35	1289	54.9	2.3	2.2	1567.74	GS	1.1	355
Hadi et al. [24]	73024	37	1200	50	2.4	1.6	759.68	GS	2.1	1220
Hadi et al. [24]	73024	37	1200	50	2.4	1.6	759.68	GS	2.1	781
Hadi et al. [24]	73024	37	1200	50	2.4	1.6	759.68	GS	2.1	494
Hadi et al. [24]	73024	37	1200	50	2.4	1.6	759.68	GS	4.2	1309
Hadi et al. [24]	73024	37	1200	50	2.4	1.6	759.68	GS	4.2	767
Hadi et al. [24]	73024	37	1200	50	2.4	1.6	759.68	GS	4.2	479
Hadi and Youssef [48]	44100	29.3	1641	67.9	2.41	1	506.45	GH	2.74	1285
Hadi and Youssef [48]	44100	29.3	1641	67.9	2.41	1	506.45	GH	2.74	803
Hadi and Youssef [48]	44100	29.3	1641	67.9	2.41	1	506.45	GH	2.74	615
Hassan et al. [49]	17662	40	800	30	0.97	2.1	425.08	SS	1.7	426.59
Hassan et al. [49]	17662	40	800	30	1.35	2.1	425.08	SS	1.7	411.88
Hassan et al. [49]	17662	40	800	30	1.57	2.1	425.08	SS	1.7	387.36
Hassan et al. [49]	17662	40	800	30	1.4	2.1	425.08	SS	3.4	529.56
Hassan et al. [49]	17662	40	800	30	1.7	2.1	425.08	SS	3.4	490.33
Hassan et al. [49]	17662	40	800	30	1.9	2.1	425.08	SS	3.4	460.91
Hassan et al. [49]	17662	40	800	30	1.28	2.1	425.08	GH	1.7	490.33
Hassan et al. [49]	17662	40	800	30	1.5	2.1	425.08	GH	1.7	460.91
Hassan et al. [49]	17662	40	800	30	1.7	2.1	425.08	GH	1.7	430.4
Karim et al. [50]	32989	37	1600	66	2.42	4.72	759.68	GS	1.91	1425
Karim et al. [50]	32989	37	1600	66	2.42	4.72	759.68	GS	3.82	2041
Karim et al. [51]	33312	37	1600	66	2.42	4.72	759.68	GS	1.91	1425
Karim et al. [51]	33636	37	1600	66	2.42	4.72	759.68	GS	1.91	781
Karim et al. [51]	33962	37	1600	66	2.42	4.72	759.68	GS	1.91	494
Karim et al. [51]	34289	37	1600	66	2.42	4.72	759.68	GS	3.82	2041

Karim et al. [51]	34618	37	1600	66	2.42	4.72	759.68	GS	3.82	767
Karim et al. [51]	34948	37	1600	66	2.42	4.72	759.68	GS	3.82	479
Karim et al. [51]	35281	37	1600	66	2.42	4.72	759.68	GS	1.91	3068
Karim et al. [51]	35614	37	1600	66	2.42	4.72	759.68	GS	1.91	1450
Karim et al. [51]	35949	37	1600	66	2.42	4.72	759.68	GS	1.91	805
Khan et al. [52]	33312	37	1395	56	1.5	3.57	1175.80	GH	-	2812
Khan et al. [52]	33312	37	1395	56	1.5	3.57	1175.80	GH	-	1487
Khan et al. [52]	33312	37	1395	56	1.5	3.57	1175.80	GH	-	910
Khorramian & Sadeghian [53]	22500	37	629	38.7	1.62	5.3	1175.80	N	-	775
Khorramian & Sadeghian [53]	22500	37	629	38.7	1.62	5.3	1175.80	N	-	775
Khorramian & Sadeghian [53]	22500	37	629	38.7	1.62	5.3	1175.80	N	-	693
Khorramian & Sadeghian [53]	22500	37	629	38.7	1.62	5.3	1175.80	N	-	693
Khorramian & Sadeghian [53]	22500	37	629	38.7	1.62	5.3	1175.80	N	-	693
Khorramian & Sadeghian [53]	22500	37	629	38.7	1.62	5.3	1175.80	N	-	578
Khorramian & Sadeghian [53]	22500	37	629	38.7	1.62	5.3	1175.80	N	-	578
Khorramian & Sadeghian [53]	22500	37	629	38.7	1.62	5.3	1175.80	N	-	354
Khorramian & Sadeghian [53]	22500	37	629	38.7	1.62	5.3	1175.80	N	-	354
Maranan et al. [54]	49062	34.42	1184	62.6	1.89	2.43	1175.80	N	-	1772
Maranan et al. [54]	49062	34.42	1184	62.6	1.89	2.43	1175.80	GH	3.13	1791
Maranan et al. [54]	49062	34.42	1184	62.6	1.89	2.43	1175.80	GH	1.57	1981
Maranan et al. [54]	49062	34.42	1184	62.6	1.89	2.43	1175.80	GH	0.78	1988
Maranan et al. [54]	49062	34.42	1184	62.6	1.89	2.43	1175.80	GS	3.13	1838
Maranan et al. [54]	49062	34.42	1184	62.6	1.89	2.43	1175.80	GS	1.57	2063
Maranan et al. [54]	49062	34.42	1184	62.6	1.89	2.43	1175.80	GH	1.57	1624
Maranan et al. [54]	49062	34.42	1184	62.6	1.89	2.43	1175.80	GS	1.57	1208
Mohamed et al. [55]	70650	42.9	934	55.4	1.56	2.2	1567.74	GH	2.23	2840
Mohamed et al. [55]	70650	42.9	934	55.4	1.56	2.2	1567.74	GH	2.68	2871
Mohamed et al. [55]	70650	42.9	934	55.4	1.56	2.2	1567.74	GH	3.14	2935
Pantelides et al. [56]	50645.06	36	740	43.3	1.71	1.6	783.87	GS	0.75	1975
Pantelides et al. [56]	50645.06	36	740	43.3	1.71	1.6	783.87	GS	0.75	1788
Prachasaree et al. [57]	22500	20.8	735	50	1.5	1.4	283.39	SS	0.01	370
Prachasaree et al. [57]	22500	20.8	735	50	1.5	1.4	283.39	SS	0.01	370
Prachasaree et al. [57]	22500	20.8	735	50	1.5	1.4	283.39	SS	0.01	370
Prachasaree et al. [57]	22500	20.8	735	50	1.5	1.4	283.39	SS	0.02	365
Prachasaree et al. [57]	22500	20.8	735	50	1.5	1.4	283.39	SS	0.02	365
Prachasaree et al. [57]	22500	20.8	735	50	1.5	1.4	283.39	SS	0.02	365
Prachasaree et al. [57]	17662	20.8	735	50	1.5	1.9	283.39	SS	0.01	345
Prachasaree et al. [57]	17662	20.8	735	50	1.5	1.9	283.39	SS	0.01	345
Prachasaree et al. [57]	17662	20.8	735	50	1.5	1.9	283.39	SS	0.01	345
Prachasaree et al. [57]	17662	20.8	735	50	1.5	1.9	283.39	SS	0.02	315
Prachasaree et al. [57]	17662	20.8	735	50	1.5	1.9	283.39	SS	0.02	315

Prachasaree et al. [57]	17662	20.8	735	50	1.5	1.9	283.39	SS	0.02	315
Prachasaree et al. [57]	22500	20.8	735	50	1.5	1.4	283.39	SH	0.01	365
Prachasaree et al. [57]	22500	20.8	735	50	1.5	1.4	283.39	SH	0.01	365
Prachasaree et al. [57]	22500	20.8	735	50	1.5	1.4	283.39	SH	0.01	365
Prachasaree et al. [57]	22500	20.8	735	50	1.5	1.4	283.39	SH	0.02	370
Prachasaree et al. [57]	22500	20.8	735	50	1.5	1.4	283.39	SH	0.02	370
Prachasaree et al. [57]	22500	20.8	735	50	1.5	1.4	283.39	SH	0.02	370
Sankholkar et al. [58]	32349.	50	800	46.2	1.57	2.5	783.87	GS	3.2	1353
Sankholkar et al. [58]	32349.	50	800	46.2	1.57	2.5	783.87	GS	3.2	1285
Sankholkar et al. [58]	32349.	50	800	46.2	1.57	3.7	1175.80	GS	3.2	1623
Sankholkar et al. [58]	32349.	50	800	46.2	1.57	3.7	1175.80	GS	3.2	1570
Sun et al. [59]	22500	23.51	1103	54.1	1.5	1.04	425.08	SH	0.63	201
Sun et al. [59]	22500	23.51	1103	54.1	1.5	1.04	425.08	SH	0.63	174
Sun et al. [59]	22500	23.51	1103	54.1	1.5	1.04	425.08	SH	0.63	181
Sun et al. [59]	22500	23.51	1103	54.1	1.5	1.04	425.08	SH	0.63	291
Sun et al. [59]	22500	23.51	1103	54.1	1.5	1.04	425.08	SH	0.63	290
Sun et al. [59]	22500	23.51	1103	54.1	1.5	1.04	425.08	SH	0.63	347
Sun et al. [59]	22500	23.51	1103	54.1	1.5	1.04	425.08	SH	0.63	632
Sun et al. [59]	22500	23.51	1103	54.1	1.5	1.04	425.08	SH	0.63	677
Sun et al. [59]	22500	23.51	1103	54.1	1.5	1.04	425.08	SH	0.63	602
Tikka et al. [60]	22500	25.7	630	40	1.5	2.3	506.45	CS	0.33	401
Tikka et al. [60]	22500	25.7	630	40	1.5	2.3	506.45	CS	0.33	120
Tikka et al. [60]	22500	25.7	630	40	1.5	3.4	759.68	CS	0.33	215
Tikka et al. [60]	22500	25.7	630	40	1.5	3.4	759.68	CS	0.33	114
Tikka et al. [60]	22500	25.7	630	40	1.5	2.3	506.45	CS	0.33	382
Tikka et al. [60]	22500	25.7	630	40	1.5	2.3	506.45	CS	0.33	129
Tikka et al. [60]	22500	25.7	630	40	1.5	3.4	759.68	CS	0.33	220
Tikka et al. [60]	22500	25.7	630	40	1.5	3.4	759.68	CS	0.33	116
Tobbi et al. [61]	122500	32.6	728	47.6	1.53	1.9	2267.08	GH	2	3929
Tobbi et al. [61]	122500	32.6	728	47.6	1.53	1.9	2267.08	GH	2	3991
Tobbi et al. [61]	122500	32.6	728	47.6	1.53	1.9	2550.47	GH	1.7	4006
Tobbi et al. [61]	122500	32.6	752	48.2	1.56	1.9	2351.61	GH	3.2	3938
Tobbi et al. [61]	122500	32.6	751	48.2	1.56	1.9	2351.61	GH	4.8	4067
Tobbi et al. [61]	122500	36.4	750	48.2	1.56	1.9	2267.08	GH	2.55	4297
Tobbi et al. [61]	122500	36.4	749	48.2	1.56	1.9	2351.61	GH	3.41	4615
Tobbi et al. [61]	122500	36.4	748	48.2	1.56	1	1290.32	GH	2.55	4212
Tobbi et al. [61]	122500	36.4	747	48.2	1.56	0.8	1012.90	GH	2.55	3900
Tu et al. [62]	40000	32.1	660	44.25	1.52	1.1	506.45	GH	5.3	970.9
Tu et al. [62]	40000	32.1	660	44.25	1.52	1.1	506.45	GH	3.1	951.6
Tu et al. [62]	40000	32.1	660	44.25	1.52	1.1	506.45	GH	2	937.7
Tu et al. [62]	40000	32.1	735	46	1.6	0.8	283.39	GH	3.1	936.8
Tu et al. [62]	40000	32.1	660	44.25	1.52	1.5	506.45	GH	3.1	981.7
Tu et al. [62]	40000	32.1	660	44.25	1.52	1.1	506.45	GH	5.2	954
Tu et al. [62]	40000	32.1	660	44.25	1.52	1.1	506.45	GH	3	943.2
Tu et al. [62]	40000	32.1	660	44.25	1.52	1.1	506.45	GH	1.9	927.7

Xue et al. [63]	90000	39	654	39	2.1	1.3	1175.80	SH	0.37	3091
Xue et al. [63]	90000	39	654	39	2.1	1.3	1175.80	SH	0.37	2855
Xue et al. [63]	90000	39	654	39	2.1	1.3	1175.80	SH	0.37	2411
Xue et al. [63]	90000	39	654	39	2.1	1.3	1175.80	SH	0.37	1900
Xue et al. [63]	90000	39	654	39	2.1	1.3	1175.80	SH	0.37	647
Xue et al. [63]	90000	39	654	39	2.1	1.3	1175.80	SH	0.37	806
Xue et al. [63]	90000	39	654	39	2.1	1.3	1175.80	SH	0.37	1702
Xue et al. [63]	90000	40.3	654	39	2.1	1.3	1175.80	SH	0.37	1678
Xue et al. [63]	90000	40.3	654	39	2.1	1.3	1175.80	SH	0.37	1632
Xue et al. [63]	90000	40.3	654	39	2.1	1.3	1175.80	SH	0.37	1500
Xue et al. [63]	90000	40.3	654	39	2.1	1.3	1175.80	SH	0.37	1300
Xue et al. [63]	90000	40.3	654	39	2.1	0.9	783.87	SH	0.37	1564
Xue et al. [63]	90000	40.3	729	44	2.1	2.6	2267.08	SH	0.37	1823
Xue et al. [63]	90000	29.1	654	39	2.1	1.3	1175.80	SH	0.37	1025
Xue et al. [63]	90000	55.2	654	39	2.1	1.3	1175.80	SH	0.37	2191
Youssef and Hadi [64]	44100	29.3	405.9	23.4	1.8	1.15	506.45	GH	2.24	1285
Youssef and Hadi [64]	44100	29.3	405.9	23.4	1.8	1.15	506.45	GH	2.24	803
Youssef and Hadi [64]	44100	29.3	405.9	23.4	1.8	1.15	506.45	GH	2.24	615
Zhang and Deng [65]	122500	42.5	840	45	1.87	1.39	1567.74	GH	1.8	5670
Zhang and Deng [65]	122500	42.5	840	45	1.87	1.39	1567.74	GH	1.8	4585
Zhang and Deng [65]	122500	42.5	840	45	1.87	1.39	1567.74	GH	1.8	5361
Zhang and Deng [65]	122500	42.5	840	45	1.87	1.39	1567.74	GH	2.7	5205
Zhang and Deng [65]	122500	42.5	840	45	1.87	1.39	1567.74	GH	2.7	5357
Zhang and Deng [65]	122500	42.5	840	45	1.87	1.39	1567.74	GH	2.7	4852
Zhang and Deng [65]	122500	42.5	840	45	1.87	2.09	2351.61	GH	2.49	4500
Zhang and Deng [65]	122500	42.5	840	45	1.87	2.64	2351.61	GH	2.49	4972

2.1.2. Assessment of previous models and new model

To predict ALC for FRP-RCS, twelve models (Table 2) were evaluated. This assessment was carried out with the help of different statistical measures e.g., the sum of squared error (*SSE*), the root mean squared error (*RMSE*), the coefficient of determination (R^2), while R^2 being the most significant indicator for the best fit analysis. These statistical indices are presented below:

$$R^2 = \left(\frac{n(\sum_{i=1}^{n} x_i y_i) - (\sum_{i=1}^{n} x_i)(\sum_{i=1}^{n} y_i)}{\sqrt{[n\sum_{i=1}^{n} x_i{}^2 - (\sum_{i=1}^{n} x_i)^2][n\sum_{i=1}^{n} y_i{}^2 - (\sum_{i=1}^{n} y_i)^2]}} \right)^2 \quad (1)$$

$$SSE = \frac{1}{n}\sum_{i=1}^{n} |x_i - y_i| \quad (2)$$

$$RMSE = \sqrt{\frac{1}{n}\sum_{i=1}^{n} (x_i - y_i)^2} \quad (3)$$

Table 2. The ALC models utilized for assessment purpose

Research/standard	Equation/model
ACI 318-11 [34]	$P_n = 0.85f_c'(A_g - A_s)$
CSA S806-02 [35]	$P_n = 0.85f_c'(A_g - A_{FRP})$
CSA S806-12 [66]	$P_n = \alpha_1 f_c'(A_g - A_{FRP});\ \alpha_1 = 0.85 - 0.0015f_c' \geq 0.67$
AS-3600 [67]	$P_n = 0.85f_c'(A_g - A_{FRP}) + 0.0025E_{FRP}A_{FRP}$
Afifi et al. [21]	$P_n = 0.85f_c'(A_g - A_{FRP}) + \alpha_g f_{FRP}A_{FRP}\ ;\ \alpha_g = 0.35$
Hadi et al. [24]	$P_n = 0.90f_c'(A_g - A_{FRP}) + \varepsilon_{fg}E_{FRP}A_{FRP}\ ;\ \varepsilon_{fg} = 0.003$
Tobbi et al. [22]	$P_n = 0.85f_c'(A_g - A_{FRP}) + \varepsilon_{co}E_{FRP}A_{FRP};\ \varepsilon_{co} = 0.003$
Samani and Attard [68]	$P_n = 0.85f_c'(A_g - A_{FRP}) + 0.0025E_{FRP}A_{FRP}$
Hadhood et al. [69]	$P_n = \alpha_1 f_c'(A_g - A_{FRP}) + 0.0035E_{FRP}A_{FRP};\ \alpha_1 = 0.85 - 0.0015f_c'$
Khan et al. [70]	$P_n = 0.85f_{cc}'(A_g - A_{GFRP}) + \alpha f_{GFRP}A_{GFRP};\ \alpha = 0.61$
Mohamed et al. [32]	$P_n = 0.85f_c'(A_g - A_{FRP}) + \varepsilon_p E_{FRP}A_{FRP};\ \varepsilon_p = 0.002$
Pantelides et al. [16]	$P_n = 0.85f_{ccFRP}'A_c + A_{FRP}\varepsilon_{cFRP}E_{FRP};\ \varepsilon_{cFRP} = 0.003$

Here, *x* being the testing parameter for FPL, *y* is considered as the prediction factor, whereas n is the total number of data sets. It is obvious that prediction accuracy gets increased when R^2 gets closer to 1. The statistical details of the predictions of various models are presented in Figure 1a-e. Figure 1a shows the minimum values of the ALC of HCCs predicted from different previous models. It can be observed that the proposed model presented the highest accuracy for predicting the lowest value of the ALC of columns with a value of 289.8 kN. Similarly, Figure 1b describes the maximum values of the ALC of HCCs predicted from different previous models. It can be observed that the model proposed by Khan et al. [70] presented the highest accuracy for predicting the highest value of the ALC of columns with a value of 15173.82 kN.

Figure 1c represents the average values of the ALC of HCCs predicted from different previous models. It can be observed that the proposed model presented the highest accuracy for predicting the average value of the ALC of columns with a value of 1783.77 kN presenting only a discrepancy of 1.73%. Figure 1d elaborates the standard deviation of the values of the ALC of HCCs predicted from different previous models. It can be observed that the proposed model presented the lowest standard deviation for predicting the lowest value of the ALC of columns with a value of 1495.6 kN. Finally, Figure 1e describes the coefficient of variation for the values of the ALC of HCCs predicted from different previous models. It can be observed that the proposed model presented the coefficient of variation of 0.84 but the model proposed by Khan et al. [70] presented the highest accuracy with the lowest value for this coefficient. Nevertheless, this model mostly overestimated the predictions for the ALC of columns.

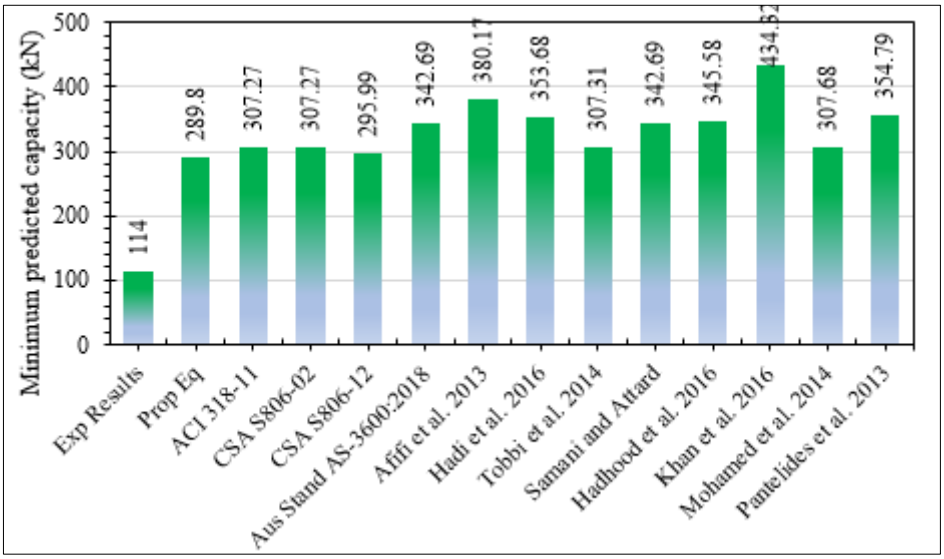

(a)

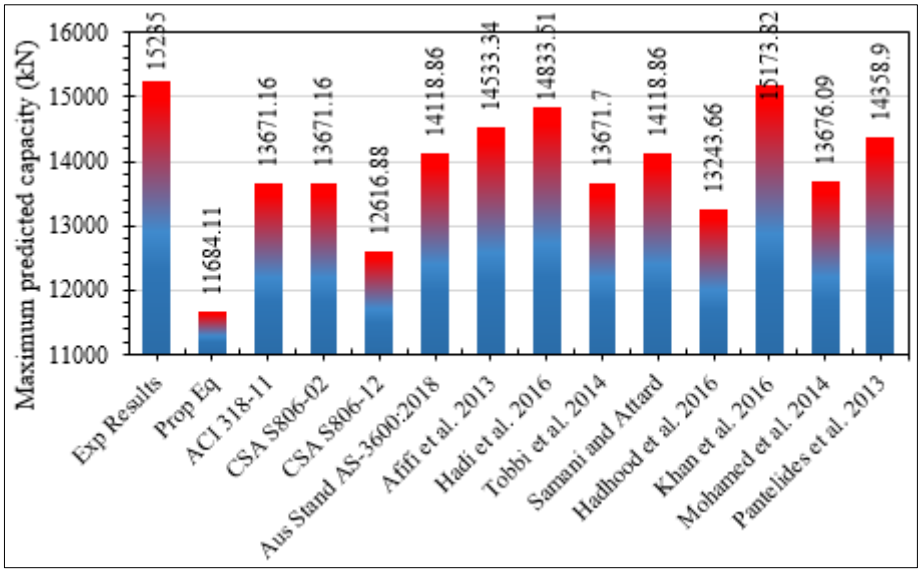
Maximum predicted capacity (kN)
16000
15000
14000
13000
12000
11000
15285
11684.11
13671.16
13671.16
12616.88
14118.86
14533.34
14833.51
13671.7
14118.86
13243.66
15173.82
13676.09
14358.9
Exp Results
Prop Eq
ACI 318-11
CSA S806-02
CSA S806-12
Aus Stand AS-3600:2018
Afifi et al. 2013
Hadi et al. 2016
Tobbi et al. 2014
Samani and Attard
Hadhood et al. 2016
Khan et al. 2016
Mohamed et al. 2014
Pantelides et al. 2013

(b)

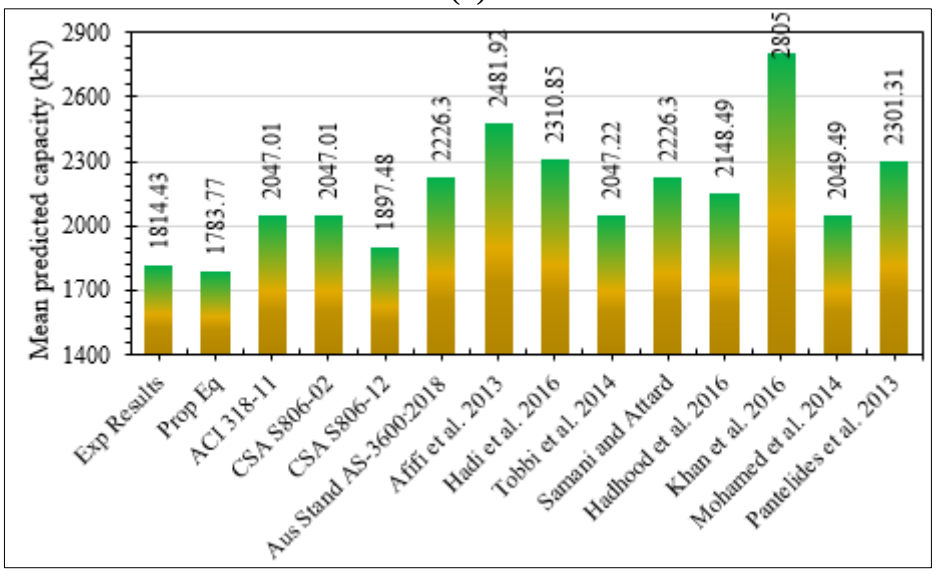
Mean predicted capacity (kN)
2900
2600
2300
2000
1700
1400
1814.43
1783.77
2047.01
2047.01
1897.48
2226.3
2481.92
2310.85
2047.22
2226.3
2148.49
2805
2049.49
2301.31
Exp Results
Prop Eq
ACI 318-11
CSA S806-02
CSA S806-12
Aus Stand AS-3600:2018
Afifi et al. 2013
Hadi et al. 2016
Tobbi et al. 2014
Samani and Attard
Hadhood et al. 2016
Khan et al. 2016
Mohamed et al. 2014
Pantelides et al. 2013

(c)

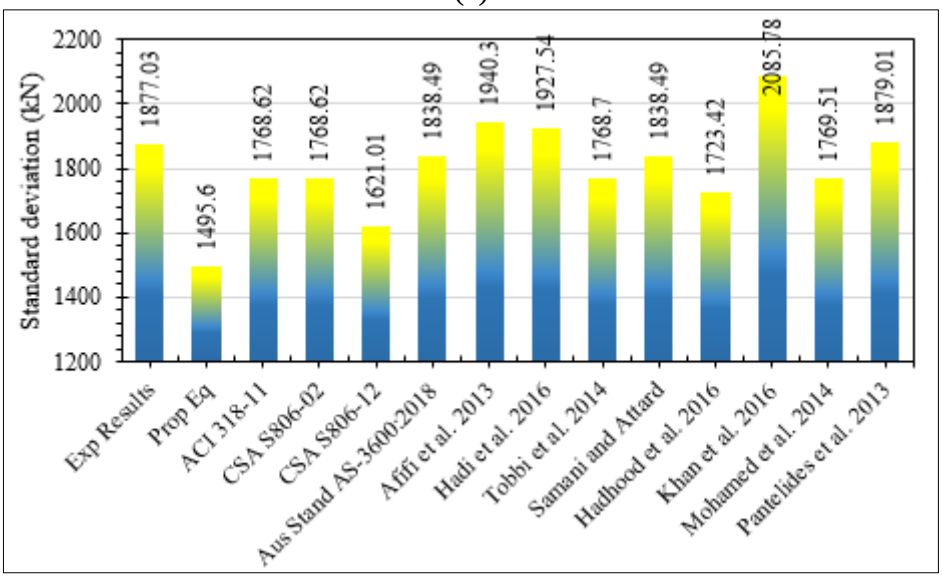
Standard deviation (kN)
2200
2000
1800
1600
1400
1200
1877.03
1495.6
1768.62
1768.62
1621.01
1838.49
1940.3
1927.54
1768.7
1838.49
1723.42
2085.78
1769.51
1879.01
Exp Results
Prop Eq
ACI 318-11
CSA S806-02
CSA S806-12
Aus Stand AS-3600:2018
Afifi et al. 2013
Hadi et al. 2016
Tobbi et al. 2014
Samani and Attard
Hadhood et al. 2016
Khan et al. 2016
Mohamed et al. 2014
Pantelides et al. 2013

(d)

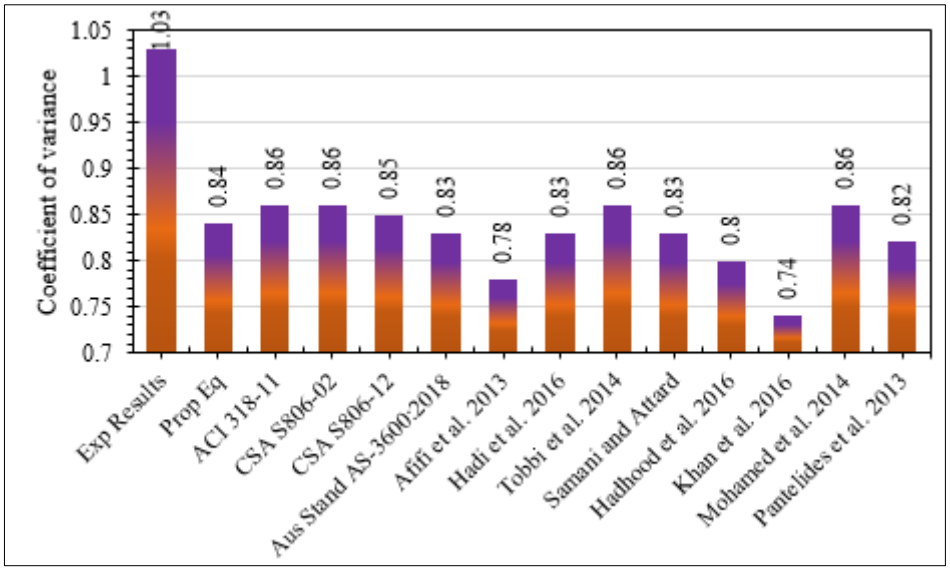

(e)

Figure 1. Statistical details of the ALC predictions of the previous models (a) minimum predicted values (b) maximum predicted values (c) average predicted values (d) standard deviations of predicted values (e) coefficient of variation for predicted values

Based on the previous models, the R^2 assessment is shown in Figure 2. The model proposed by Tobbi et al. [22] had an R^2 of 0.721. So, in general, this form of the model proposed by this study was also retained like that proposed by Tobbi et al. [22]. This model suggested the impact of FRP main rebars to be kept at that level of a maximum strain having 0.003 having reduction factor up to 35 percent. The full form of this model is given by equation (4).

$$P_{n1} = \alpha_1\left(A_g - A_{FRP}\right)f_c' + \alpha_2 E_{FRP}A_{FRP} \tag{4}$$

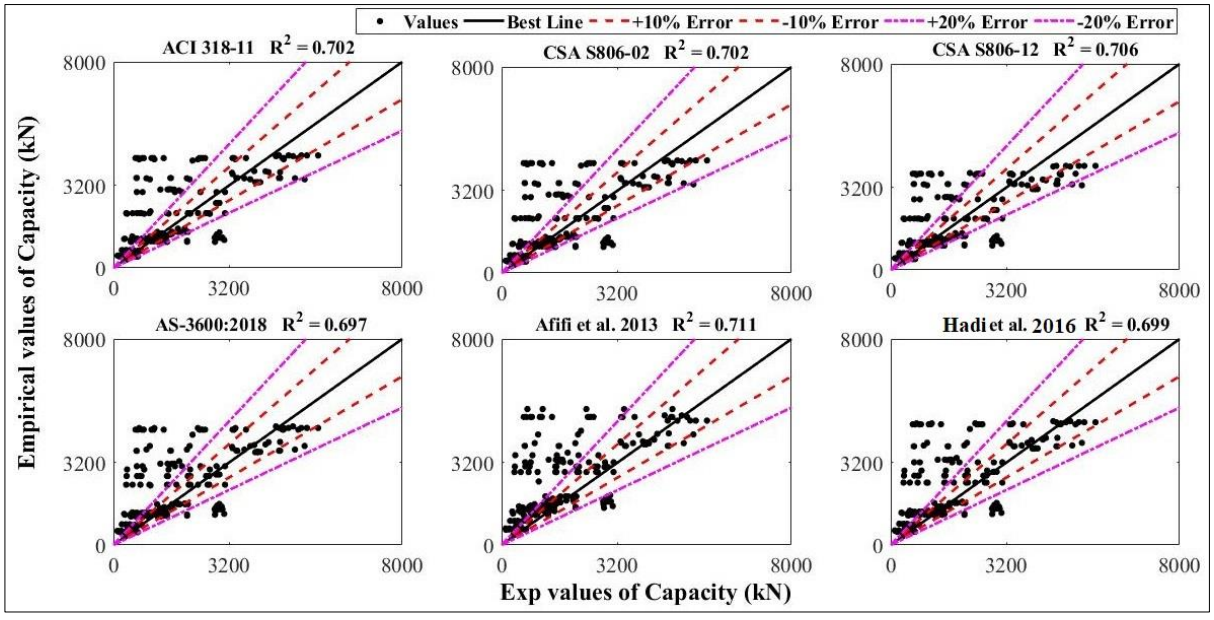

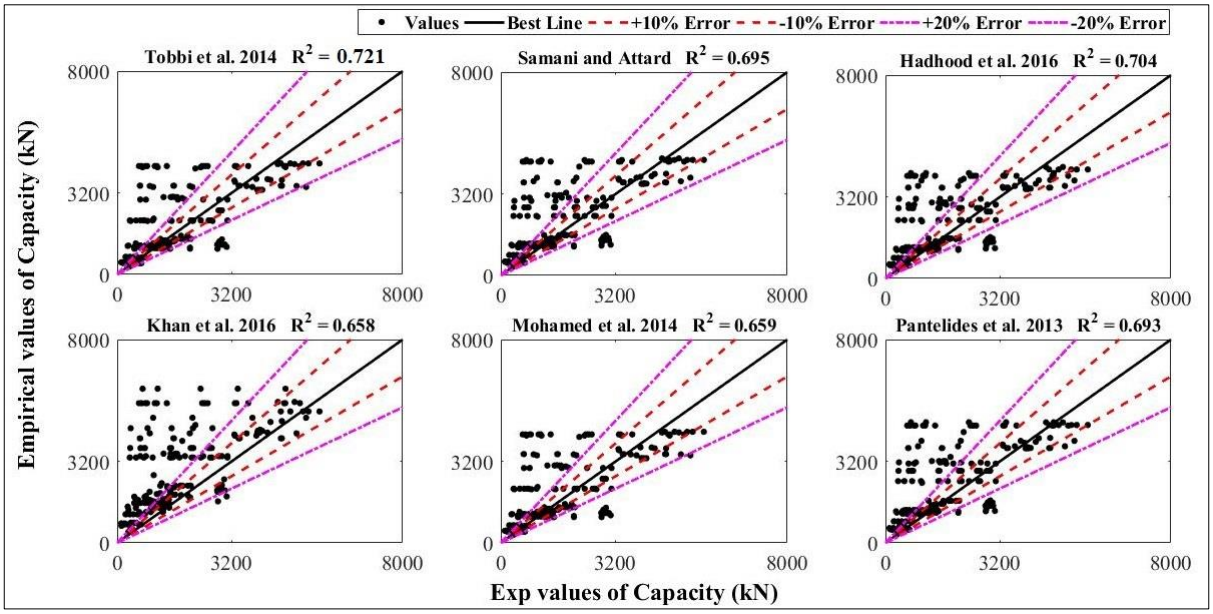

Figure 2. The pattern of ALC of FRP-RCC members

where α_1 and α_2 being the concrete reduction factors and FRP rebars contribution parameters, while A_g represents column's total CSA, f_{FRP} being the FRP strength in tension and A_{FRP} to be the gross CSA for main FRP bars. Numerical coefficients obtained by curve fittings via MATLAB helped reduce the error function for the test of the best fits. Ultimately, the recommended association for the FPL for HCCs was relying on the experimental observations collected with the database are presented by equation (5).

$$P_{n1} = (0.85 - 0.0028f_c')\left(A_g - A_{FRP}\right)f_c' + 0.0028E_{FRP}A_{FRP} \quad (5)$$

where, $\alpha_1 = 0.85 - 0.0028f_c' \geq 0.645$. With this proposed model it was found that the accuracy was more than those of all the published models, having an R^2 of 0.73 as reported in Figure 3.

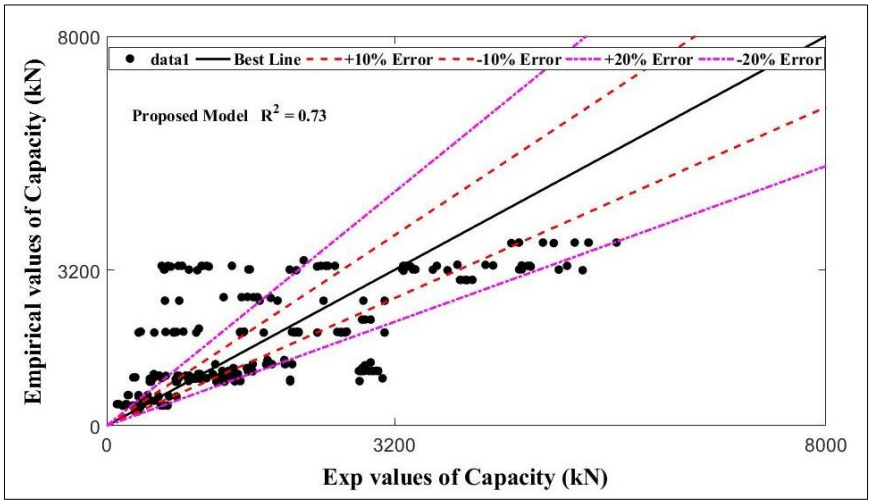

Figure 3. Proposed model behavior for the first peak loadings

With the help of experimentations and proposed models, various normal distribution plots for tested versus predicted dataset is shown in Figure 4. Based on, ratios of the mean normalized dataset of test the very FPL loading to those estimated first peaks, it is evident that the suggested model performed quite well yielding only 5 percent from unity. Whereas, this deviation was observed to be a maximum of 40% by Khan et al. [70].

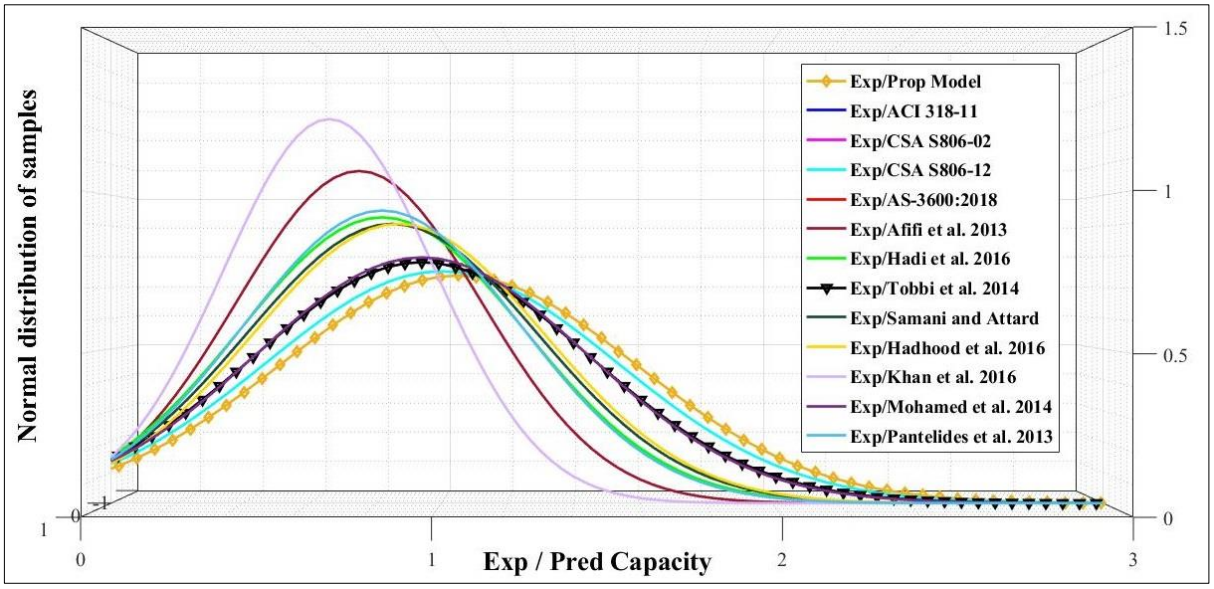

Figure 4. Normal distribution pattern of tested to estimated ALC of FRP-RCC acquired from several models

Figure 5 depicts the FPL estimates of suggested and previously proposed models for six different HCCs strengthened glass-FRP specimens [27]. Mean percent errors for the ALC models of Pantelides et al. [16], Mohamed et al. [32], Khan et al. [70], Hadhood et al. [69], Samani & Attard [68], Tobbi et al. [22], Hadi et al. [24], Afifi et al. [21], AS-3600 [67], CSA S806-12 [66], CSA S806-02 [35], and ACI 318-11 [34], were governed by the ultimate loading strength of six HCCs with 4.4, 6.4, 62.7, 3.5, 4.0, 3.5, 6.5, 27.7, 4.0, 22.93, 19.3, and 19.3%, respectively. However, Afifi et al. [21] and Khan et al. [70] miscalculated the FPL. The reason behind this deviation is keeping the influence of main glass-FRP rebars in consideration while computing the ALC of HCCs for their ultimate tensile strength estimates. On the other hand, the models in studies [34] undervalued the ALC by taking into account the influence of glass-FRP bars in the form of their strains. Likewise, it was also perceived that whenever these models utilized the strains glass-FRP rebars in the main direction, predictions were relatively more accurate. The best accurate model was found for that suggested by Tobbi et al. [22] having an average 5 error of 3.5 percent. However, the presently suggested model offered an error value up to 3.3 percent.

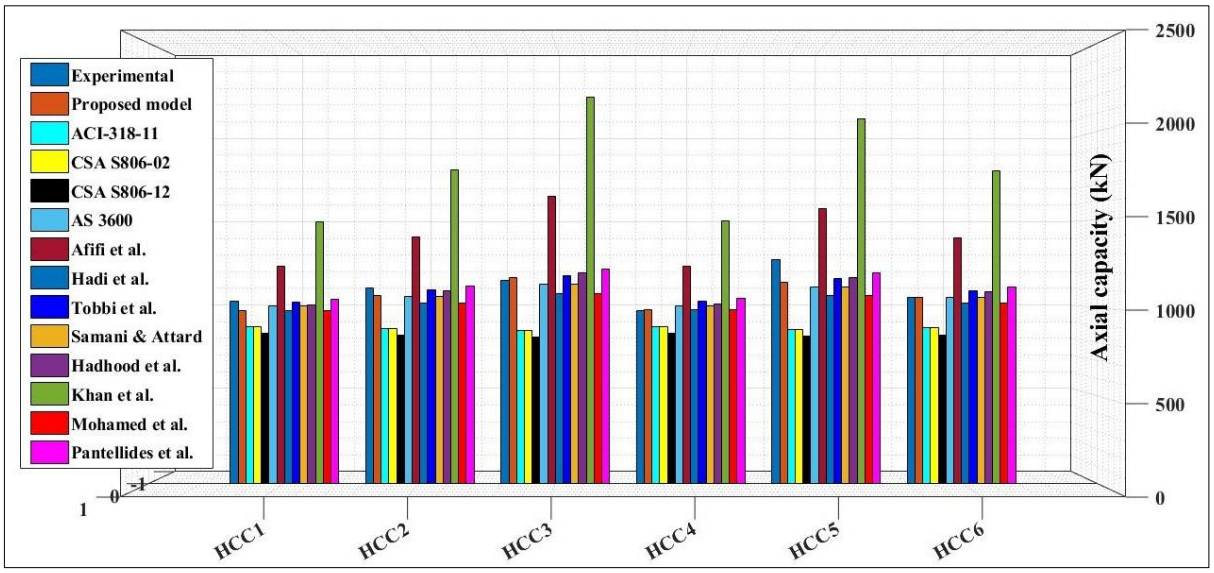

Figure 5. Estimates of six HCCs' the first peaks with suggested and previous capacity models

It is obvious with the present proposed capacity model that it yielded a closer agreement of the FPL capacity of HCCs with experimental data. This shows the reliability of the ALC estimates for HCCs by utilizing the effectiveness of glass-FRP's reinforcements with strain compatibility value up to 0.0028 with the concrete. Therefore, for estimations of FPL of glass-FRP-strengthened HCCs, the currently proposed model was found more accurate.

Second peak capacity

Approaching the FPL, the lateral glass-FRP spirals wrapping is activated during the post-loading stage. This phenomenon averts the concrete core failure and offers more bracing to the glass-FRP rebars. This process causes to experience relatively higher axial loads because of the higher strain efficacy of glass-FRP rebars in the main direction. During the process, the ALC of glass-FRP rebars increased significantly in the main direction, resulting in significant axial loadings. Whereas, during the SPL (P_{n2}) of HCCs, the main glass-FRP rebars as well as the remainder of core gets effective [27]. Similarly, the lateral confining stresses (f_l) can be computed with the help mechanical-wrapping theory [71]. Figure 6 depicts mechanical-wrapping concepts based on glass-FRP spirals.

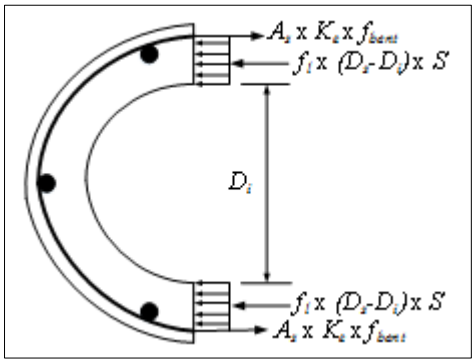

Figure 6. Mechanical wrapping effects resulting from glass-FRP spirals

$$f_l = \frac{2A_s K_\varepsilon f_{bent}}{S(D_s - D_i)} \tag{6}$$

Here, A_s being the CSA of the glass-FRP lateral wrappings, S to be the c/c distance of glass-FRP spirals, D_s be the c/c glass-FRP spirals diameter, D_i to be the diameter of the internal hollow region of HCCs, K_ε showing the mean damaging stains to be 0.533 [27], and f_{bent} showing the maximum tensile strength of bent glass-FRP computed with equation (7) as per ACI-440.1R [72]. This lateral wrapping effect resulting from glass-FRP spirals confining the concrete material partially by separating most of the concrete being unwrapped between spirals and those of main glass-FRP rebars. This partial wrapping pattern because of glass-FRP spirals has been presented in Figure 7a. Whereas, taking into account the partial transverse wrappings, an effective wrapping factor (k_e) was presented as given by equation (8) [73].

$$f_{bent} = \left(0.05\frac{r}{d_b} + 0.3\right) f_u \leq f_u \tag{7}$$

where, d_b being the diameter of glass-FRP spirals, while r to be the radius of the glass-FRP spiral.

$$k_e = \frac{A_{ce}}{A_{cc}} = \frac{\left(D_s - \frac{s'}{4}\right)^2 - D_i^2}{(D_s^2 - D_i^2)(1-\rho_e)} \tag{8}$$

In this equation, A_{ce} being the concrete core's CSA which retained concrete crushed between the distance of the spirals, s' to be the clear distance between the glass-FRP spirals, whereas A_{cc} is the CSA of core after apart from the effective glass-FRP bars (ρ_e). Because k_e the factor does not precisely represent the wrapping of glass-FRP spirals, consequently, to elaborate this process of the opening of glass-FRP spirals another factor with enhanced accuracy is introduced called (k_o). This factor (as shown by equation (9)) is considered more favorable for its use in the partial glass-FRP spirals [27]. This opening behavior of glass-FRP spirals is highlighted in Figure 7b.

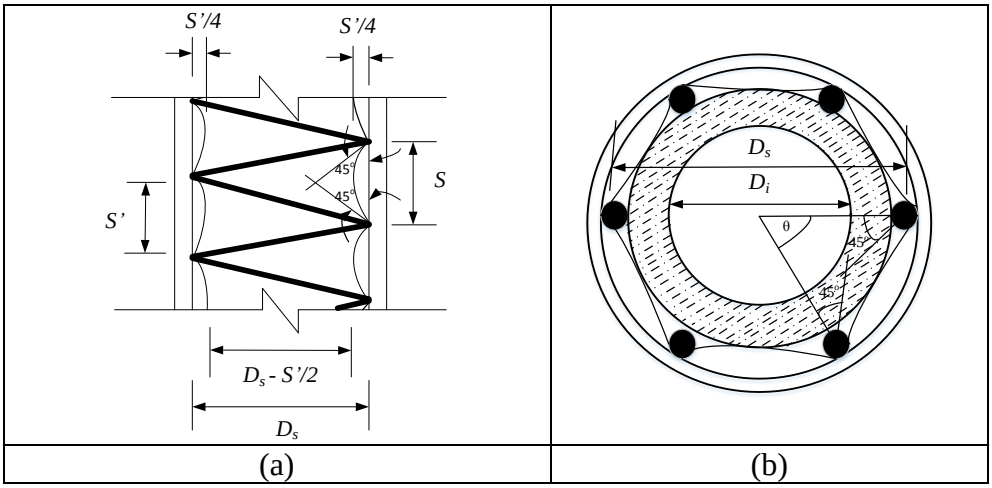

Figure 7. Wrapping mechanics (a) Wrapping pattern resulting from a vertical distance of glass-FRP spirals (b) Opening effect of glass-FRP spirals

$$k_o = \frac{A_d}{A_{cc}} = \frac{D_s^2\left(\frac{1}{2}+\frac{\cos\left(\frac{\theta}{2}\right)}{2}-\left(\frac{\sin\left(\frac{\theta}{2}\right)\tan\left(45-\frac{\theta}{2}\right)}{4}\right)\right)^2 - D_i^2}{\left(D_s^2-D_i^2\right)(1-\rho_e)} \quad (9)$$

where, A_d is the CSA of the concrete core once the crushed concrete gets removed because of the opening mechanisms of glass-FRP spiral reinforcements. While θ is the included angle between the two main but consecutive glass-FRP rebars. However, the 2nd peak capacity of HCCs also relies on the CSA of glass-FRP rebars. The HCCs strengthened with the bars of larger diameters are shown with even greater losses in the compressive strengths of the concrete core after the SPL is met [28]. In addition to this, another factor for rebar diameter (k_d) is shown by equation (10) that reflects the reduction of concrete strength and the ratio of the second moment of area of glass-FRP main rebars (I_{FRP}) to that of core ($I_{concrete}$) at the SPL stage [27].

$$k_d = 1.215 \times e^{-2400\times\frac{I_{FRP}}{I_{concrete}}} \quad (10)$$

Resulting in, the lateral wrapping (f_l) gets converted to effective lateral wrapping (f_{le}) being equal to the f_l times k_d, and the larger of either k_o or k_e subjected to factor controlling the partial damaging patterns. Accordingly, the SPL capacity of HCCs may be thought of as a relationship of experimented core strength (f_{ce}) of concrete presented with equation (11) by Alajarmeh et al. [27]. Lastly, the SPL capacity of HCCs (P_{n2}) computed via eq. (12) by taking into account the impact of glass-FRP reinforcements in the form of axial strains at SPL up to 0.011 [27] and the elastic modulus (E_{FRP}).

$$f_{ce} = 3.69\{\max(k_e, k_o) \times k_d \times f_l\} + 1.03 \quad (11)$$

$$P_{n2} = f_{ce}A_{cc} + 0.011E_{FRP}A_{FRP} \quad (12)$$

Figure 8 presents the comparison of the experimental SPL values for six HCCs with their predicted values. It also shows that the proposed model accurately anticipated the P_{n2} of HCCs. The average difference (%) between the tested outcomes and the modeled theoretical estimates was 6.5 percent. Thus, the proposed model may be utilized to accurately forecast the SPL capacity of HCCs with glass-FRP.

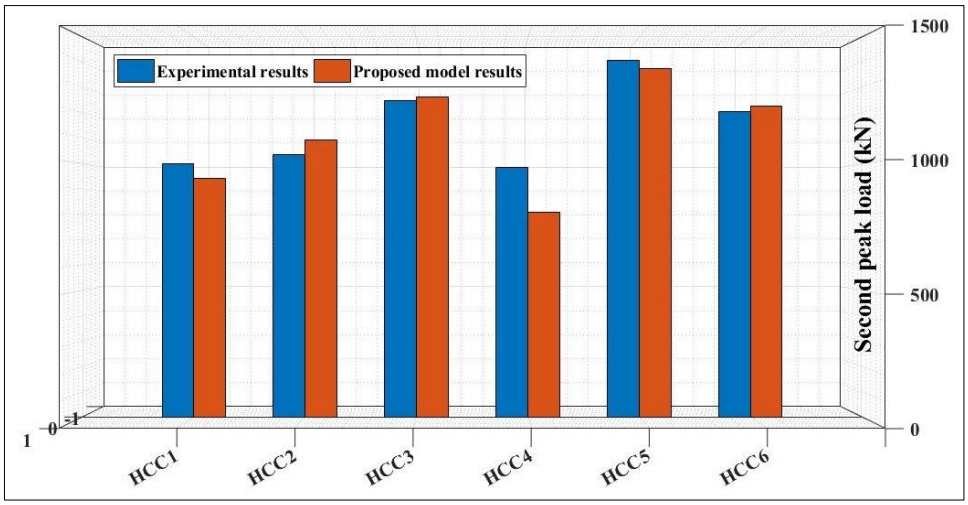

Figure 8. Estimates of second peaks of six HCCs with the presently proposed model

4.Conclusions

HCCs are efficient structural members that are light in weight with greater stiffness and stability. The present work has endeavored to assess the theoretical capacity of glass-FRP-reinforced HCCs. Two different models were suggested to capture the two-peak behaviors of HCCs established with a detailed database developed with the help of published literature. The comparison of the predictions of proposed models portrayed that they could capture the FPL and SPL pattern of glass-FRP-strengthened HCCs with higher accuracy. This research could help structural engineers simulate, analyze, and design HCCs with glass-FRP reinforcement in severely corrosive conditions. The following are the core points of the research:

-for forecasting axial ALC of glass-FRP-RCC hollow columns, the influence of glass-FRP rebars with concrete is essential. The axial contributions of glass-FRP bars in the form of their peak tensile strength overestimated the results. Whereas, the impact of glass-FRP rebars in the form of their peak strain underestimated the predictions. However, such impact in the form of strains presented a better performance to estimate the ALC of HCCs;

-the newly developed model to estimate the FPL capacity of glass-FRP-strengthened HCCs established with the database of two hundred and seventy-nine FRP-RCCs specimens performed well with R^2 of 0.73 that is portraying more accuracy than the models available in the literature. The suggested model for the FPL of HCCs denoted by discrepancy (%) of 3.3 founded on the experimental outcomes of 6 HCCs by utilizing the axial strains of 0.002 in glass-FRP rebars;

-while predicting the first peak load, the reduction factor for the ALC due to concrete should be $\alpha_1 = 0.85 - 0.0028 f_c' \geq 0.645$.

-likewise, the SPL capacity of glass-FRP-RCC hollow columns can be precisely anticipated by taking into account the compressive strain of 0.011. Similarly, for the SPL, the mean discrepancy of theoretical outcomes from the tested outcomes was found to be 6.54% only. The provided theoretical models for the two peaks are realistic enough to predict the peak loadings of glass-FRP-reinforced HCCs, notwithstanding these slight deviations.

Acknowledgments: The Authors extend their appreciation to the Deanship of Scientific Research at King Khalid University for funding this work through the Large Groups Project under grant number R.G.P. 2/5/43"

References

1.KUSUMAWARDANINGSIH, Y., HADI, MNS., Comparative behaviour of hollow columns confined with FRP composites. *Composite Structures*, 2010. 93(1): p. 198-205.
2.LIGNOLA, G.P., PROTA, A., MANFREDI, G., COSENZA, E., Experimental performance of RC hollow columns confined with CFRP. *Journal of Composites for Construction,* 2007. 11(1): p. 42-49.
3.LIGNOLA, G.P., NARDONE, F., PROTA, A., DE LUCA, A., NANNI, A., Analysis of RC hollow columns strengthened with GFRP. *Journal of Composites for Construction*, 2010. 15(4): p. 545556.
4.HOSHIKUMA, J., PRIESTLEY, MJN., Flexural behavior of circular hollow columns with a single layer of reinforcement under seismic loading. *SSRP*, 2000. 13.
5.LEE, J.H., CHOI, J.H., HWANG, D.K., KWAHK, I.J., Seismic performance of circular hollow RC bridge columns. *KSCE Journal of Civil Engineering*, 2015. 19(5): p. 1456-1467.
6.YEH, Y., MO, YL., YANG, CY., Seismic performance of hollow circular bridge piers. *Structural Journal*, 2001. 98(6): p. 862-871.
7.YEH, Y., MO, YL., YANG, CY., Seismic performance of rectangular hollow bridge columns. *Journal of Structural Engineering*, 2002. 128(1): p. 60-68.
8.PAVESE, A., BOLOGNINI, D., PELOSO, S., FRP seismic retrofit of RC square hollow section bridge piers. *Journal of earthquake engineering*, 2004. 8(spec01): p. 225-250.
9.OSADA, K., YAMAGUCHI, T., IKEDA, S., Seismic performance and the strengthening of hollow circular RC piers having reinforced cut-off planes and variable wall thickness. *Concrete Res. and Tech*, 1999. 101: p. 13-24.
10.MO, Y., WONG, DC., MAEKAWA, K., Seismic performance of hollow bridge columns. *Structural Journal*, 2003. 100(3): p. 337-348.
11.PINTO, A., MOLINA, J., TSIONIS, G., Cyclic tests on large-scale models of existing bridge piers with rectangular hollow cross-section. *Earthquake engineering & structural dynamics*, 2003. 32(13): p. 1995-2012.
12.ZAHN, F., PARK, R., PRIESTLEY, MJN., Flexural strength and ductility of circular hollow reinforced concrete columns without confinement on inside face. *Structural Journal*, 1990. 87(2): p. 156-166.
13.HADI, M., LE, TD., Behaviour of hollow core square reinforced concrete columns wrapped with CFRP with different fibre orientations. *Construction and Building Materials*, 2014. 50: p. 62-73.
14.YAZICI, V., Strengthening hollow reinforced concrete columns with fibre reinforced polymers. 2012.
15.LI, J., GONG, J., WANG, L., Seismic behavior of corrosion-damaged reinforced concrete columns strengthened using combined carbon fiber-reinforced polymer and steel jacket. *Construction and Building Materials*, 2009. 23(7): p. 2653-2663.
16.PANTELIDES, C.P., GIBBONS, M.E., REAVELEY, L.D., Axial load behavior of concrete columns confined with GFRP spirals. *Journal of Composites for Construction*, 2013. 17(3): p. 305-313.
17.RAHAI, A., AKBARPOUR, H., Experimental investigation on rectangular RC columns strengthened with CFRP composites under axial load and biaxial bending. *Composite Structures,* 2014. 108: p. 538-546.
18.MATTHYS, S., TOUTANJI, H., AUDENAERT, K., TAERWE, L., Axial load behavior of large-scale columns confined with fiber-reinforced polymer composites. *ACI Structural Journal,* 2005. 102(2): p. 258.
19.HADI, M., Behaviour of FRP wrapped normal strength concrete columns under eccentric loading. *Composite Structures,* 2006. 72(4): p. 503-511.

20.ZENG, J.J., LV, J.F., LIN, G., GUO, Y.C., LI, L.J., Compressive behavior of double-tube concrete columns with an outer square FRP tube and an inner circular high-strength steel tube. *Construction and Building Materials*, 2018. 184: p. 668-680.
21.AFIFI, M.Z., MOHAMED, H. M., BENMOKRANE, B., Axial capacity of circular concrete columns reinforced with GFRP bars and spirals. *Journal of Composites for Construction*, 2013. 18(1): p. 04013017.
22.TOBBI, H., FARGHALY, A.S., BENMOKRANE, B., Behavior of Concentrically Loaded Fiber-Reinforced Polymer Reinforced Concrete Columns with Varying Reinforcement Types and Ratios. *ACI Structural Journal*, 2014. 111(2).
23.MARANAN, G., MANALO, AC., BENMOKRANE, B., KARUNASENA, W., MENDIS, P., Behavior of concentrically loaded geopolymer-concrete circular columns reinforced longitudinally and transversely with GFRP bars. *Engineering Structures*, 2016. 117: p. 422-436.
24.HADI, M., KARIM, H., SHEIKH, MN., Experimental investigations on circular concrete columns reinforced with GFRP bars and helices under different loading conditions. *Journal of Composites for Construction*, 2016. 20(4): p. 04016009.
25.HADI, M., HASAN, HA., SHEIKH, MN., Experimental investigation of circular high-strength concrete columns reinforced with glass fiber-reinforced polymer bars and helices under different loading conditions. *Journal of Composites for Construction*, 2017. 21(4): p. 04017005.
26.HADHOOD, A., MOHAMED, H.M., BENMOKRANE, B., Experimental study of circular high-strength concrete columns reinforced with GFRP bars and spirals under concentric and eccentric loading. *Journal of Composites for Construction*, 2016. 21(2): p. 04016078.
27.ALAJARMEH, O., MANALO, AC., BENMOKRANE, B., KARUNASENA, W., MENDIS, P., Axial performance of hollow concrete columns reinforced with GFRP composite bars with different reinforcement ratios. *Composite Structures*, 2019. 213: p. 153-164.
28.ALAJARMEH, O., MANALO, AC., BENMOKRANE, B., KARUNASENA, W., MENDIS, P., NGUYEN, KTQ., Compressive behavior of axially loaded circular hollow concrete columns reinforced with GFRP bars and spirals. *Construction and Building Materials*, 2019. 194: p. 12-23.
29.HADHOOD, A., ET AL., Efficiency of glass-fiber reinforced-polymer (GFRP) discrete hoops and bars in concrete columns under combined axial and flexural loads. *Composites Part B: Engineering*, 2017. 114: p. 223-236.
30.KARIM, H., SHEIKH, M.N., HADI, MNS., Axial load-axial deformation behaviour of circular concrete columns reinforced with GFRP bars and helices. *Construction and Building Materials*, 2016. 112: p. 1147-1157.
31.RAZA, A., KHAN, QUZ, AHMAD, A., Numerical investigation of load-carrying capacity of GFRP-reinforced rectangular concrete members using CDP model in ABAQUS. Advances in Civil Engineering, 2019. 2019.
32.MOHAMED, H.M., AFIFI, M.Z., BENMOKRANE, B., Performance evaluation of concrete columns reinforced longitudinally with FRP bars and confined with FRP hoops and spirals under axial load. *Journal of Bridge Engineering*, 2014. 19(7): p. 04014020.
33.AFIFI, M.Z., MOHAMED, H.M., BENMOKRANE, B., Theoretical stress–strain model for circular concrete columns confined by GFRP spirals and hoops. *Engineering Structures*, 2015. 102: p. 202-213.
34.***ACI 318-11, Guide for the design and construction of externally bonded FRP systems for strengthening concrete structures. Americ Concr Instit; Farmington Hills, MI, U.S.A. 2011.
35.***Association, C.S., Canadian highway bridge design code-Section 16).CAN/CSA-S6-02, Toronto. 2002.
36.AFIFI, M.Z., H.M. MOHAMED, AND B. BENMOKRANE, Axial capacity of circular concrete columns reinforced with GFRP bars and spirals. *Journal of Composites for Construction*, 2014. 18(1): p. 04013017.

37.AFIFI, M.Z., H.M. MOHAMED, AND B. BENMOKRANE, Theoretical stress–strain model for circular concrete columns confined by GFRP spirals and hoops. *Engineering Structures*, 2015. 102: p. 202-213.
38.ALAJARMEH, O., ET AL., Compressive behavior of axially loaded circular hollow concrete columns reinforced with GFRP bars and spirals. *Construction and Building Materials,* 2019. 194: p. 12-23.
39.ALAJARMEH, O.S., ET AL., Axial performance of hollow concrete columns reinforced with GFRP composite bars with different reinforcement ratios. *Composite Structures,* 2019. 213: p. 153-164.
40.ALSAYED, S., ET AL., Concrete columns reinforced by glass fiber reinforced polymer rods. *Special Publication*, 1999. 188: p. 103-112.
41.DE LUCA, A., F. MATTA, A. NANNI, Behavior of full-scale glass fiber-reinforced polymer reinforced concrete columns under axial load. *ACI structural journal*, 2010. 107(5): p. 589.
42.DONG, M., ET AL., Glass fibre-reinforced polymer circular alkali-activated fly ash/slag concrete members under combined loading. *Engineering Structures*, 2019. 199: p. 109598.
43.ELCHALAKANI, M., G. MA, Tests of glass fibre reinforced polymer rectangular concrete columns subjected to concentric and eccentric axial loading. *Engineering Structures,* 2017. 151: p. 93-104.
44.GUÉRIN, M., ET AL., Eccentric Behavior of Full-Scale Reinforced Concrete Columns with Glass Fiber-Reinforced Polymer Bars and Ties. *ACI Structural Journal*, 2018. 115(2).
45.GUÉRIN, M., ET AL., Effect of glass fiber-reinforced polymer reinforcement ratio on axial-flexural strength of reinforced concrete columns. *ACI Structural Journal*, 2018. 115(4): p. 1049-3.
46.HADHOOD, A., H.M. MOHAMED, B. BENMOKRANE, Axial load–moment interaction diagram of circular concrete columns reinforced with CFRP bars and spirals: Experimental and theoretical investigations. *Journal of Composites for Construction*, 2017. 21(2): p. 04016092.
47.HADHOOD, A., H.M. MOHAMED, B. BENMOKRANE, Assessing stress-block parameters in designing circular high-strength concrete members reinforced with FRP bars. *Journal of Structural Engineering*, 2018. 144(10): p. 04018182.
48.HADI, M.N. AND J. YOUSSEF, Experimental investigation of GFRP-reinforced and GFRP-encased square concrete specimens under axial and eccentric load, and four-point bending test. *Journal of Composites for Construction*, 2016. 20(5): p. 04016020.
49.HASSAN, A., ET AL., Structural behaviour of self-compacting concrete columns reinforced by steel and glass fibre-reinforced polymer rebars under eccentric loads. *Engineering Structures*, 2019. 188: p. 717-728.
50.KARIM, H., M.N. SHEIKH, M.N. HADI, Axial load-axial deformation behaviour of circular concrete columns reinforced with GFRP bars and helices. *Construction and Building Materials*, 2016. 112: p. 1147-1157.
51.KARIM, H., M. NEAZ SHEIKH, M.N. HADI, Load and moment interaction diagram for circular concrete columns reinforced with GFRP bars and GFRP helices. *Journal of Composites for Construction*, 2017. 21(1): p. 04016076.
52.KHAN, Q.S., M.N. SHEIKH, M.N. HADI, Axial-flexural interactions of GFRP-CFFT columns with and without reinforcing GFRP bars. *Journal of composites for construction,* 2017. 21(3): p. 04016109.
53.KHORRAMIAN, K., P. SADEGHIAN, Experimental and analytical behavior of short concrete columns reinforced with GFRP bars under eccentric loading. *Engineering structures,* 2017. 151: p. 761-773.
54.MARANAN, G., ET AL., Behavior of concentrically loaded geopolymer-concrete circular columns reinforced longitudinally and transversely with GFRP bars. *Engineering Structures,* 2016. 117: p. 422-436.
55.MOHAMED, H.M., M.Z. AFIFI, B. BENMOKRANE, Performance evaluation of concrete columns reinforced longitudinally with FRP bars and confined with FRP hoops and spirals under axial load. *Journal of Bridge Engineering*, 2014. 19(7): p. 04014020.

56.PANTELIDES, C.P., M.E. GIBBONS, L.D. REAVELEY, Axial load behavior of concrete columns confined with GFRP spirals. *Journal of Composites for Construction*, 2013. 17(3): p. 305-313.
57.PRACHASAREE, W., ET AL., Behavior and performance of GFRP reinforced concrete columns with various types of stirrups. *International Journal of Polymer Science*, 2015. 2015.
58.SANKHOLKAR, P.P., C.P. PANTELIDES, AND T.A. HALES, Confinement model for concrete columns reinforced with GFRP spirals. *Journal of Composites for Construction*, 2018. 22(3): p. 04018007.
59.SUN, L., M. WEI, N. ZHANG, Experimental study on the behavior of GFRP reinforced concrete columns under eccentric axial load. *Construction and Building Materials*, 2017. 152: p. 214-225.
60.TIKKA, T., M. FRANCIS, B. TENG. Strength of concrete beam-columns reinforced with GFRP bars. in 2nd International Structures Specialty Conference, Winnipeg, MB, Canada. 2010.
61.TOBBI, H., A.S. FARGHALY, B. BENMOKRANE, Concrete Columns Reinforced Longitudinally and Transversally with Glass Fiber-Reinforced Polymer Bars. *ACI Structural Journal*, 2012. 109(4).
62.TU, J., ET AL., Experimental study on the axial compression performance of GFRP-reinforced concrete square columns. *Advances in Structural Engineering*, 2019. 22(7): p. 1554-1565.
63.XUE, W., F. PENG, Z. FANG, Behavior and design of slender rectangular concrete columns longitudinally reinforced with fiber-reinforced polymer bars. *ACI Structural Journal*, 2018. 115(2): p. 311-322.
64.YOUSSEF, J., M.N. HADI, Axial load-bending moment diagrams of GFRP reinforced columns and GFRP encased square columns. *Construction and Building Materials*, 2017. 135: p. 550-564.
65.ZHANG, X., Z. DENG, Experimental study and theoretical analysis on axial compressive behavior of concrete columns reinforced with GFRP bars and PVA fibers. *Construction and Building Materials*, 2018. 172: p. 519-532.
66.***Association, C.S., Design and construction of building structures with fibre-reinforced polymer, CAN/CSA S806-12. Toronto, ON, Canada. 2012.
67.***Standard, A., Australian Standard 3600: concrete structures. Standards Australia. 2018.
68.SAMANI, A.K., ATTARD, M.M., A stress–strain model for uniaxial and confined concrete under compression. *Engineering Structures*, 2012. 41: p. 335-349.
69.HADHOOD, A., MOHAMED, H.M., BENMOKRANE, B., Axial load–moment interaction diagram of circular concrete columns reinforced with CFRP bars and spirals: Experimental and theoretical investigations. *Journal of Composites for Construction*, 2016. 21(2): p. 04016092.
70.KHAN, Q.S., SHEIKH, M.N., HADI, MNS., Axial-flexural interactions of GFRP-CFFT columns with and without reinforcing GFRP bars. *Journal of composites for construction*, 2016. 21(3): p. 04016109.
71.HAN, T., LIM, NH, HAN, SY, PARK, JS, KANG, YJ, Nonlinear concrete model for an internally confined hollow reinforced concrete column. *Magazine of Concrete Research*, 2008. 60(6): p. 429-440.
72.SAADATMANESH, H., M.R. EHSANI, AND M.-W. LI, Strength and ductility of concrete columns externally reinforced with fiber composite straps. *Structural Journal*, 1994. 91(4): p. 434-447.
73.MANDER, J., PRIESTLEY, MJN, PARK, R, Behaviour of ductile hollow reinforced concrete columns. *Bulletin of the New Zealand National Society for Earthquake Engineering*, 1983. 16(4): p. 273-290.

Manuscript received: 18.04.2022